

## Article

# A Methodological Tool to Assess Erosion Susceptibility of High Coastal Sectors: Case Studies from Campania Region (Southern Italy)

Maria Francesca Tursi <sup>1</sup>, Giorgio Anfuso <sup>2,\*</sup>, Fabio Matano <sup>3</sup>, Gaia Mattei <sup>1</sup> and Pietro P. C. Aucelli <sup>1</sup>

<sup>1</sup> Department of Science and Technology, University of Naples Parthenope, Centro Direzionale, Isola C4, 80121 Napoli, Italy

<sup>2</sup> Department of Earth Sciences, Faculty of Marine and Environmental Sciences, University of Cádiz, 11510 Puerto Real, Spain

<sup>3</sup> National Research Council, Institute of Marine Sciences (CNR-ISMAR), 80133 Napoli, Italy

\* Correspondence: giorgio.anfuso@uca.es; Tel.: +34-956-016167

**Abstract:** High coastal sectors constitute the most widespread coastal environment and, under the present accelerated sea-level rise scenario, are suffering huge impacts in terms of erosion. The aim of this paper is the proposal of a new methodological approach for the assessment of their susceptibility to erosive processes. The method is based on the combination of two matrices, i.e., a matrix considering the main physical elements (essentially morphological and geotechnical characteristics) that determine the proneness to erosion of a specific high coastal sector, and a forcing matrix, which describes the forcing agents affecting the considered sector. Firstly, several variables were selected to construct each one of the two matrices according to existing studies and, in a second step, they were interpolated to obtain the susceptibility matrix (CSIx). The approach was applied to Procida Island and Cilento promontory, both located in southern Italy. Results obtained were validated by comparing them with cliff retreat data obtained by means of aerial photographs and satellite images. The analysis shows that the greater part of the analyzed high coastal sectors belongs to the high-susceptibility class due to the combination of adverse morphological, geotechnical and forcing characteristics. Such sectors can be considered “hotspots” that require an increase in monitoring programs and, at places, urgent protective actions.

**Keywords:** geomorphology; high coast; susceptibility index; relative sea level rise; Cilento; Procida Island



**Citation:** Tursi, M.F.; Anfuso, G.; Matano, F.; Mattei, G.; Aucelli, P.P.C. A Methodological Tool to Assess Erosion Susceptibility of High Coastal Sectors: Case Studies from Campania Region (Southern Italy). *Water* **2023**, *15*, 121. <https://doi.org/10.3390/w15010121>

Academic Editors: Trilochan Sahoo, Swaroop Nandan Bora and Santanu Koley

Received: 30 November 2022

Revised: 21 December 2022

Accepted: 22 December 2022

Published: 29 December 2022



**Copyright:** © 2022 by the authors. Licensee MDPI, Basel, Switzerland. This article is an open access article distributed under the terms and conditions of the Creative Commons Attribution (CC BY) license (<https://creativecommons.org/licenses/by/4.0/>).

## 1. Introduction

High coasts, which include sea cliffs, bluffs and rocky shore platforms [1], are the most widespread geomorphic coastal environment, occurring along about 80% of the world's shoreline [2,3]. In Europe, coastal cliffs, which human occupation has been continuously growing in the last decades, represent 11.7% of the length of the whole shoreline, with 3620 km eroding, 970 km artificially protected, and 380 km both protected and eroding [4]. Under the present accelerated sea-level rise scenario, these landforms are suffering huge impacts in terms of erosion. It is often assumed that climate change and, in particular, sea level rise, will lead to higher rates of erosion of high coastal sectors [5], as it can change the frequency and duration of the direct impacts of waves on them, usually the primary agents controlling cliff evolution [6].

In particular, cliff erosion takes place through a combination of marine and terrestrial processes and depends on cliff-forming materials (i.e., rock type, structural weaknesses, presence of groundwater, for example), as well as physical forces such wave energy, tidal range, degree of protection offered by beach or protection structures, local climate, and frequency and magnitude of severe storm events [6].

The interaction of these complex mechanisms results in an increase in erosion rates—with cliff erosion usually observable in the form of mass movement [7]. Cliff retreat represents an episodic, very difficult observing and measuring issue: it often takes place at high rates during low-frequency events, e.g., high-energy storms produce episodic erosion higher than the average retreat recorded during years or decades [8]. Despite all of the above, the greater part of the existing studies on coastal processes have traditionally been focused on low sandy coasts [9–15].

The analysis and evaluation of coastal susceptibility is a highly debated topic since many factors and variables (both natural and human-related) determine coastal behavior. In order to carry out suitable protection actions, coastal managers need to know the physical susceptibility of the investigated environments and future socio-economic impacts [10,16–19]. In response to this necessity, various authors proposed new methodologies for the characterization of coastal areas according to their susceptibility/vulnerability and/or hazard criteria [1,20–22].

In Italy, Budetta et al. [23] proposed a heuristic method for landslide hazard zonation along the coastal bluffs and cliffs of the Cilento area (southern Italy) by the computation of an Instability Index, while De Pippo et al. [21] proposed a semiquantitative method to quantify, rank and map the spatial distribution of coastal hazards along the northern part of the Campania region. In the Campi Flegrei area, the multi-temporal analysis of Terrestrial Laser Scanning (TLS) datasets and digital elevation models (DEMs), derived from existing aerial images and airborne LIDAR data processing, were aimed at evaluating geostructures, geomorphic evolution, and cliff retreat rates of the Coroglio tuff cliff in Naples [24,25] and of the Torrefumo cliff (during the 1956–2016 period), in Monte di Procida [26,27]. The monitoring of a large rockslide evolution at the Baia dei Porci cliff, in the Monte di Procida area, was carried out by using the “Structure-from-Motion” (SfM) photogrammetry technique [28]. De Vita et al. [29] carried out, along the eastern part of Liguria region, an engineering and geological analysis of the rock failure susceptibility of a high rocky coast using non-contact geostructural surveys, while Di Luccio et al. [30] presented a methodology based on hydraulic and geomorphological characteristics along Procida’s high coasts (Campania region). In addition, Lucchetti et al. [31] tested, along a Ligurian coastal sector, a method to elaborate geomorphological hazard and risk mapping of rocky coasts by applying a new classification system (Sea Cliff Mass Rating-SCMR) based on a modification of the Slope Mass Rating index (SMR) [32]. Along the Slovenian coast, Furlani et al. [33] tested an integrated method to evaluate cliff retreat and the factors triggering the collapse of material and its removal from the cliff foot joining a detailed characterization of the geomechanical properties and the quality of rock masses, the susceptibility to rock fall processes, and photographic surveying.

In a coastal sector of Cadiz province (SW Spain), Del Rio & Gracia [1] proposed a method to evaluate cliff erosion risk, allowing the zoning of a coastal cliffed area according to the cliff erosion hazard, the influence of erosion and the risk for the area. In the same area, Anfuso et al. [34] tested a methodological approach to determine cliff characteristics and the probability of collapse by using Bieniawski’s method [35] and considering the role of cliff verticality and the presence/absence of protective structures. Rangel-Buitrago & Anfuso [19] used an index-based method to determine: (i) the susceptibility of low sand and high rocky coasts to storm impacts taking into account their physical parameters; (ii) coastal vulnerability, taking into account socio-economic activities, ecological and cultural heritage, and (iii) the associated risk.

In Portugal, Marques et al. [36] undertook a statistically-based study to assess the capacity of a set of conditioning factors to express the occurrence of sea cliff failures at a regional scale. In the same country, Nunes et al. [37] presented an expeditive method to assess hazard in rock cliffs by combining cliff evolution forcing mechanisms along with protection factors according to a weighted factors system.

The aim of this work is the proposal of a new methodological approach for the assessment of erosion susceptibility of cliffed coastal sectors through an indices-based method.

This approach requires the selection and evaluation of several geomorphological, geotechnical, and forcing/dynamic variables involved in the determination of the susceptibility to erosion of high coastal sectors. The proposed method does not present a score based on the frequency or magnitude of erosive events but furnishes a grade of proneness of cliffed coastal environment to erosion.

The proposed index-based method was applied along several high coastal sectors located in the Cilento and Procida areas, both in the Campania region (southern Italy). The studied areas are popular tourist destinations that are especially frequented during the summer period, i.e., from June to August. The two areas differ in their geological, geomorphological and forcing/dynamic settings, and support different levels of human occupation.

The proposed index-based method, tested and corroborated through comparison with real calculated data on cliff erosion, is valid for the classification of a wide range of cliffed areas placed in temperate and equatorial environments. The resulting information will be of primary importance for implementing adequate land use planning and management strategies, especially in less developed coastal areas.

## 2. Study Area

The methodological approach proposed for the determination of the susceptibility index has been tested along different high coastal sectors in the Cilento area and Procida Island, both located in the Campania region of southern Italy, and characterized by a semidiurnal microtidal environment (tidal range < 2 m).

### 2.1. Cilento Area

The Cilento area is located in the southern part of the Campania region between the Gulf of Salerno to the North and the Alento plain to the South [38], Figure 1A, and is over 45 km in length, extended along a wide rectangular promontory [39]. This coastal area is characterised by a diversity of landforms and environments: zones of high rocky coast, such as those of Agropoli and San Marco di Castellabate, where massive cliffs are often associated with abrasion platforms at their base, are alternated with low coastal zones such as those of Santa Maria di Castellabate and Ogliastro Marina, where alluvial plains meet the sea, giving rise to bays and well-developed beaches. High coastal sectors in this area, showing a height usually ranging from 5 to 55 m, are mainly composed of stratified sandstones with marls and conglomerates belonging to the Cilento group [40–43].

Most cliffs are located on the back of wide shore platforms and support a great variety of uses, from highly urbanized areas to protected, well-preserved, marine/land areas. The area is subject to winds and waves that mainly approach from the WSW and WNW, and extreme waves reach maximum values of between 6 and 7 m.

### 2.2. Procida Island

Procida Island is located along the western sector of the Gulf of Pozzuoli, in the northern part of the Campania region (Figure 1B), which extends for ca. 2 km in width and 3 km in the SW-NE direction, covering an area of ca. 130 km<sup>2</sup> with an overall flat morphology [30,44,45]. The island has a volcanic origin and its formation is linked to several monogenic eruptions, and is prevalently explosive, which determined the formation of five volcanic centres that characterised the emerged and submerged morphology of the area [46–48]. The island is essentially characterized by high-slope cliffs alternated with sectors presenting low slope values (30–40°), while a smaller portion of the coast consists of pocket beaches limited by fossil marine promontories [47].

Concerning the cliffed sectors, two types can be distinguished according to the classification proposed by Sunamura [49], i.e., cliffs with sloping shore platforms (Type A) and subvertical cliffs in deep water (plunging cliffs). High coastal sectors observed in this area are cut into pyroclastic deposits showing a height ranging from 10 to 40 m and an inclination > 40°. Procida is exposed to winds and waves approaching from the WSW

and WNW (between  $250^{\circ}$  N and  $290^{\circ}$  N), with the highest waves reaching a maximum value  $> 6$  m [48].

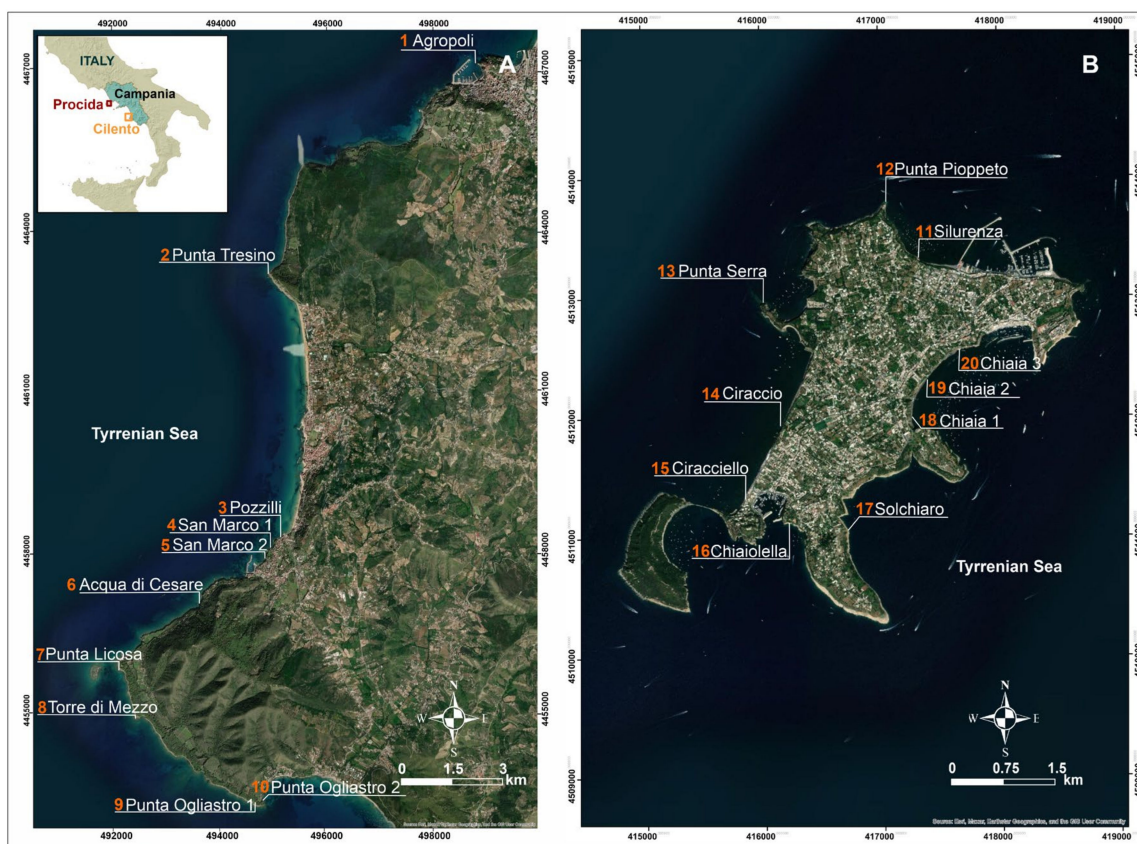


**Figure 1.** Location map of the 10 sites investigated along the Cilento coast (A) and the 10 sites located along the island of Procida (B).

### 3. Materials and Methods

The proposed method for the susceptibility assessment of high coasts has been based on the combination of two matrices:

- The physical elements matrix, the variables of which describe the proneness of cliffed coasts to erosion according to their specific morphological, geomechanical and protective characteristics
- The Forcing matrix, the variables of which describe the forcing agents affecting the coast, e.g., waves, tide, degree of littoral exposition to wavefronts, and relative sea level trend.

For each matrix, a specific index has been generated, i.e., the Physical Elements Index ( $PEI_x$ ) and the Forcing Index ( $CFI_x$ ). The selection of most of the variables used in both indices has been made following previous studies that were mainly focused on high coast resilience, sea level rise-related hazards [8,10,18,49,50], and/or storm impacts [19,51,52]. The selection of variables has been carried out following two principles. Firstly, the number of chosen variables should be maintained low enough in order to avoid redundancy problems, i.e., some variables can be closely related and reflect the same processes. Secondly, the selected variables must be available and easy to obtain in any given area, obviating the need for exhaustive survey work, as suggested by Villa & McLeod [53]. In this way, the proposed method is very practical and simple to apply in any coastal area with comparable available datasets.

Each index was divided into five different classes in a manner such that all possible cases that can be found at any cliff located in temperate and tropical climates would fall

into one of the considered classes [1]. Classes were defined following a numerical basis where possible and, for unquantifiable variables, a semi-quantitative strategy was adopted using an ordinal scale. The classes of every variable were then ranked from 1 to 5, i.e., from the lowest to the highest proneness (and forcing) value. In the following step, variables were weighted with factors (weight factor,  $W_{fi}$ ) according to their relative importance in determining the total cliff erosion hazard and forcing impact [54] in order to prevent the underestimation of the most significant variables at the local level and the overestimation of the less significant ones, and to increase the discriminating power of the method. Although the weighting of the variables is recognized as a necessity in many coastal classification studies [10], the establishment of the weight of each variable remains a difficult task since its precise role in determining cliff erosion is not easy to evaluate. As a consequence, it is clear that subjective decisions, based on professional judgments, and implicated in weighting processes represent a complex issue [55]. Therefore, when the variable considered describes a process/aspect not very important in cliff susceptibility (or is not a determinant forcing agent) its value is multiplied by 0.5 (minimum impact), while if the variable describes a common process/aspect, its value is multiplied by 0.8 (medium impact). Finally, if the variable describes a process/aspect greatly affecting cliff susceptibility (or forcing effects), its value is multiplied by 1 (maximum impact).

### 3.1. Physical Elements Index

According to the aforementioned principles, 16 factors (including variables and sub-variables) have been chosen to determine the Physical Elements Index ( $PEI_x$ ). It defines cliff proneness to coastal erosion, which is here considered as the occurrence of a number of physical, geological and geomorphological conditions inducing the coastal system to erosion [14]. Table 2 shows the classes and ranking criteria adopted for each variable, taking into account that a score of 1 represents the lowest value and 5 the highest one. The description of the parameters used in the index was presented in the following manner:

1. Cliff Height (classes modified from Gerivani et al. [56]). High cliffs have greater potential instability with respect to low ones. Therefore, the higher the class value is, the higher is the possibility of landslide occurrence, and vice versa [57].
2. Cliff Slope (Classes from Rangel-Buitrago & Anfuso [19]). Slope is considered to be directly linked to cliff instability. The higher the slope, the higher is the potential instability [21,58].
3. Cliff Lithology (and compressive strength) (classes modified from Hoek et al. [59]). Lithology and rock strength are significant factors that determine cliff erosion and instability. This parameter takes into account all of the possible types of rocks forming cliffs ranging from low to high sensible lithologies [2,54,60,61].
4. Layer Dip and Strike (classes modified from Terzaghi [62]). The dip is the angle of inclination of the rock strata with respect to the horizontal plane. Steep cliffs generally show rocks that are either vertically or horizontally bedded, whereas intermediate bed angles tend to produce more moderate slopes [2,6].
5. Erosional Landforms. Mass movements in high coastal sectors are influenced by increases in basal and superficial erosion processes related to marine and terrestrial agents. In particular:
  - a. Marine landforms (classes modified from Trenhaile [63]). These features are related to marine erosion processes at the cliff foot. The main agents are abrasion, biological activity, solution by ocean water, and quarrying of blocks [2]. Relatively fast marine erosion produces overstepping at the cliff foot, which leads to rock falls, slumps, and other kinds of mass movements.
  - b. Terrestrial Landforms (classes modified from De Pippo et al. [21]). Subaerial erosion takes the form of gulling and rain-wash at the ground surface due to slumping and other mass movements induced by groundwater [64].
6. Structure Discontinuities (Classes modified from De Pippo et al. [21]). Structures include strata, fractures, etc. and often play a key role in determining cliff evolution

since they reduce the total strength of the rocky massif. Since the approach proposed in this paper pretends to be fast and easy to apply, the complete method proposed by Bieniawski [35] is not applicable, as it requires extensive and very detailed field evaluations. Consequently, a simplified version of the Bieniawski classification [35] was applied. The used parameters were:

- a. Discontinuities Presence/Abundance. It deals with the presence/absence and abundance of discontinuities.
- b. Discontinuities Persistence. It is defined as the extension of a discontinuity in relation to a reference line that belongs to the plane in which the discontinuity is located.
- c. Discontinuities Aperture. It represents the distance between the walls of a discontinuity. They may be: closed (rock-rock contact), open or mixed (ca. 50% open and 50% closed).
- d. Discontinuities Filling. The presence of fill material in fractures increases cliff instability. This parameter considers the type of infilling, i.e., hard or soft infilling. Due to different conditions, infilled discontinuities exhibit a wide range of physical behaviors, particularly in terms of shear strength, deformability and permeability.

Vegetation Cover (Classes modified from De Pippo et al. [21]). The presence of vegetation on the cliff top is considered to play a protective role in the regulation of evapotranspiration, superficial runoff and infiltration processes [23]. In addition, its occurrence also decreases the rain impact on the cliff top and the development of root systems plays a stabilizing role as they increase the tensile strength of the rock masses; therefore, vegetation cover represents a natural stabilizing factor [65].

7. Beach. The presence of a beach facing the cliff dissipates wave energy and protects the cliff from wave action. It is important to distinguish:
  - a. Beach Type (Classes from Del Río & Gracia [1]). Beach height and width play a significant role, considering that a narrow and/or low beach allows the waves to reach the cliff foot. Since waves transport sediments, their mechanical erosion effects on the cliff foot increase [49,59,61]. Therefore, the ranking of this variable is based on the frequency with which waves reach the cliff foot—which depends on beach characteristics.
  - b. Sediment Grain Size (Classes from Mooser et al. [66]): The size of beach sediments restricts their transport and, therefore, a gravelly beach is much more stable than a sandy one. [67].
8. Shore Platform (classes modified from Sunamura [49]). The presence of a rocky shore platform located at the foreshore, or shoreface, controls the dissipation of wave energy protecting the cliff base from erosion processes. The protective effect of the shore platform depends on its width, but also its continuity and location. This variable describes three main types of cliffed coasts based on the profile shape. According to this approach, a plunging cliff coast is more susceptible to erosion than a horizontal shore platform.
9. Foot Accumulation (classes modified from De Pippo et al. [21]). Cliff recession processes release deposits that are accumulated at the foot of the cliff. Such deposits, at least temporarily, provide a natural protection against sea forces [68–70], underlining the importance of longshore currents that may remove material from the cliff foot. The losses of this non-consolidated detached material allow erosion at the cliff foot to continue.
10. Coastline Protection Structures – K index (classes from Aybulatov & Artyukhin [71]). Not only natural features are involved in cliff susceptibility definition, since human components are at places relevant, i.e., the case of protection structures at the cliff foot. Mapping the level and type of shoreline protection structures and ports/harbor (i.e., coastal armouring) is a key factor in the assessment/identification of areas

recording bathers’ safety problems [72,73]. Structures such as seawalls, rock armours, revetments, gabions, and rip-raps avoid marine erosion at the cliff foot. Other types of engineering structures not positioned at the cliff foot, such as jetties or groins, are not taken into account in the index, because they do not have a direct influence on cliff erosion [21,22,74,75]. To evaluate the level of armouring, i.e., the amount of coastline protection structures and ports/harbors within a considered coastal sector, the coefficient of technogenous impact K has been used [71]. This coefficient represents the relation between the total length (I) of all man-made structures in the considered coastal sector and its length (L). Following this methodology, different categories of technogenous impact have been obtained. All the chosen variables are reported in Table 1.

**Table 1.** Physical Elements Index rating from 1—minimum (green) to 5—maximum proneness (red) to erosion.

No	Variable	Subvariable	RATING					Weight
			Null Very Low (1)	Low (2)	Medium (3)	High (4)	Very High (5)	
1	HEIGHT		0 < h ≤ 5 m	5 < h ≤ 20 m	20 < h ≤ 40 m	40 < h ≤ 60 m	h > 60 m	0.5
2	SLOPE		S ≤ 30°	30° < S ≤ 40°	40° < S ≤ 50°	50° < S ≤ 60°	S > 60°	1
3	LITHOLOGY (Uniaxial Compressive Strength)		Fresh basalt, chert, diabase, gneiss, granite, quartzite (UCS ≥ 250 MPa)	Amphibolite, sandstone, basalt, gabbro, gneiss, granodiorite, limestone, marble, rhyolite, tuff, phyllite, schist, shale (250 < UCS ≤ 50 MPa)	Claystone, coal, concrete, schist, shale, siltstone, flysch (50 < UCS ≤ 25 MPa)	Chalk, rocksalt, potash (25 < UCS ≤ 5 MPa)	Highly weathered or altered rock, volcanic ejecta (UCS < 5 MPa)	1
4	LAYER DIP AND STRIKE		Landward dip	Transversal	Horizontal	Vertical	Seaward dip	1
5a	EROSIONAL LANDFORM	Marine erosional features	Free of erosional features (usually observed in cliffs with vertical strata striking parallel to the cliff face)	cm	dm	m	Several meters-caves (usually observed in cliffs with horizontal strata)	0.5
5b		Terrestrial erosional features	Free of erosional features	Rill	Minor gullies	Possible slump scars	Stepped and gullied and slump scars	0.5
6a	STRUCTURE DISCONTINUITIES	Presence/abundance	Virtual absence of discontinuities, cracks, joints, faults (% ≤ 30%)	x	Some evidence of discontinuities cracks, faults (30 < % ≤ 60)	x	High density of discontinuities, cracks, fault (% > 60)	0.4
6b		Persistence	cm	x	dm	x	m	0.2
6c		Aperture	Closed	x	Mixed (50% open/closed)	x	Open	0.2
6d		Infilling	None	x	Hard Infilling	x	Soft Infilling	0.2
7	VEGETATION COVER		Mature, dense and undisturbed	Mature	Poor and ephemeral	Very poor	Bare	0.5
8a	BEACH FEATURES	Type	Wide/high beach (waves reach the cliff at spring tides coinciding with storm surges)	x	Narrow/low beach (waves reach the cliff during daily high tide)	x	No beach	0.5
8b		Sediment Grain size	Gravel/pebbles	x	Medium/coarse sand or mixed	x	Fine sand	0.5

Table 1. Cont.

No	Variable	Subvariable	RATING					Weight
			Null Very Low (1)	Low (2)	Medium (3)	High (4)	Very High (5)	
9	PLATFORM FEATURES	Cliff with horizontal/sloping shore platform (waves reach the cliff at spring tides coinciding with storm surges)	x	x	Cliff with narrow horizontal/sloping shore platform (waves reach the cliff)	x	Plunging cliff (Not protected by rocky shore platform)	1
10	FOOT ACCUMULATION	Old large talus well vegetated (block or sediment of different dimensions that are stables)	x	x	Fresh Talus	x	Absent (or unstable /sediment)	0.8
11	COASTLINE DEFENCE STRUCTURES	Extreme ( $K \geq 1$ )	Maximum ( $1 < K \leq 0.50$ )	Average ( $0.5 < K \leq 0.1$ )	Minimum ( $0.1 < K \leq 0.0001$ )	No structures ( $K = 0$ )		0.8

Once obtained, the scores of each variable have been summed in order to obtain an absolute value for the index by using Equation (1):

$$PEI_x = \sum_{i=1}^n \frac{PE * WFi}{nPEI} \quad (1)$$

where  $PE$  is the Physical Elements value,  $WFi$  is the weight factor and  $nPEI$  is the number of chosen variables for the index assessment.

The obtained  $PEI_x$  values, ranging between 0 and 3, were classified into five proneness classes, ranging from very low to very high, Table 2.

**Table 2.** The obtained five Physical Elements Index classes with colors—from green to red—indicating an increase of proneness to erosion.

Class	Value
Null/Very low	$0 < PEI_x \leq 0.6$
Low	$0.6 < PEI_x \leq 1.2$
Medium	$1.2 < PEI_x \leq 1.8$
High	$1.8 < PEI_x \leq 2.4$
Very high	$2.4 < PEI_x \leq 3$

### 3.2. Coastal Forcing Index

The Forcing Index was defined as the potential stress level that a given coastline could experience [19,66]. Considering the data available at the European scale, this paper considers four forcing variables: significant wave height, tidal range, degree of littoral exposition to wave fronts, and relative sea level trend (Figure 2).

(A) Significant wave height: this parameter ( $H_s$ ) is defined as the mean wave height of the highest third (33.33%) of the waves recorded in a considered period. The range of significant wave height represents an indicator of the energy of the waves and, therefore, of the potential cliff instability. High storm waves attack and erode the foot of the cliff, causing over-steepening, resulting in the total or partial collapse of the cliff and the accumulation of debris (talus) at its base.  $H_s$ , which can be obtained in different ways, is widely used in the susceptibility literature and is usually expressed as a numeric value divided into different classes [18,76]. In this study, it has been calculated through the analysis of the MEDSEA\_MULTIYEAR\_WAV\_006 wave dataset of the Mediterranean Sea Waves forecasting system (Med-Waves) [77]. This dataset contains a multi-year wave reanalysis composed of hourly wave parameters at  $1/24^\circ$  horizontal resolution, covering the Mediterranean Sea and extending up to  $18.125^\circ$  W into the Atlantic Ocean. This dataset is based on WAVE Model WAM 4.6.2 and it is easily accessible on the Copernicus Marine Service website. In

addition, at the global level, the European Centre for Medium-Range Weather Forecasts [78] usually provides a useful database service with real-time and archive forecasts, analyses, climate reanalyses, and multi-model datasets, but wave data collected in real-time can also be obtained from local buoys and stations. The methodological approach followed in this paper proposes the use of a significant wave height value corresponding to specific storm conditions for each investigated area. The first step in this direction was the determination of a wave height threshold value, i.e., the height at which erosion starts to affect the considered coastal area. Average annual and monthly winter values (i.e., from November to February) of significant wave height ( $H_s$ ) and the 99<sup>th</sup> percentile of  $H_s$  ( $H_{s,99}$ ) were used for the characterization of wave climate and the definition and description of storms by different authors [79,80]. In this paper, the  $H_{s,99}$  was used, as it is associated with the highest energetic events [19,79].

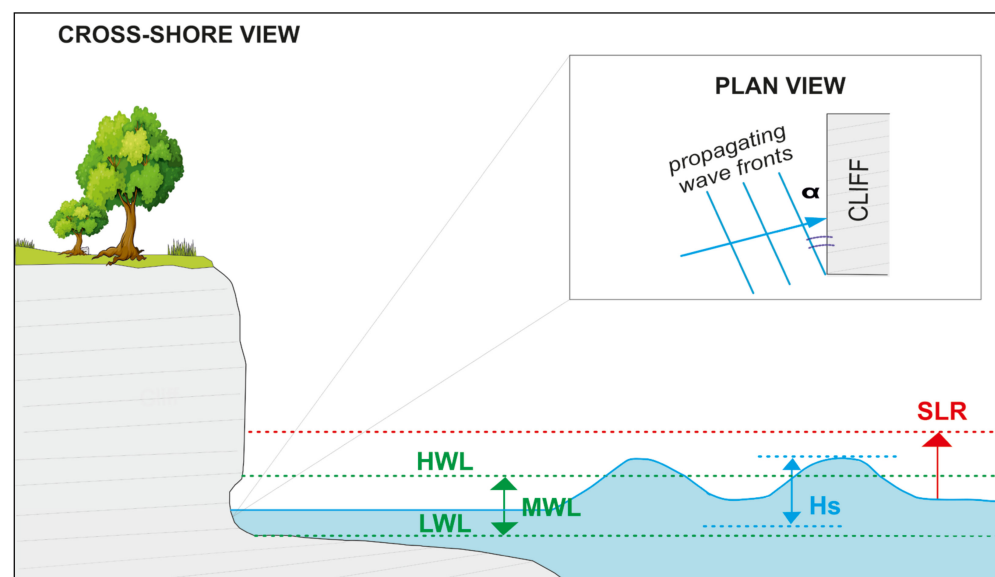


**Figure 2.** Cross-shore view of the main coastal forcing acting on a cliff.  $H_s$ : Significant wave height; MWL: Mean water level;  $\alpha$ : waves' approaching angle. It indicates the degree of littoral exposition to wave fronts; SLR: Relative Sea Level trend.

(B) Tidal range (Classes from Mclaughlin & Cooper [18]): Tides are periodic vertical movements of the sea surface of astronomic origin which depend on the configuration of oceans, bays, etc. Their associated impact is linked to the fact that tidal range determines the daily elevation of water level and the limit of the horizontal wave run-up [50]. This value, which was considered as a constant variable in local studies, included different cases, since high tidal ranks permit better dissipation of wave energy than low tidal ranks in which the erosive efficiency of waves is maximized due to their concentrated attack on a narrow vertical zone. Consequently, on cliffed sectors, higher tidal ranges are considered to imply a lower erosion hazard [67,81]. Regarding the case studies reported in this paper, they are all located in a microtidal environment.

(C) Degree of littoral exposition to wave fronts (classes from García-Mora et al. [82]): This parameter, which influences the sensitivity of the littoral to storm impacts, represents the existing angle between the coastline and the storm wavefronts, usually determined through qualitative observation. According to Komar [83], shore parallel storm wavefronts involve higher hazard levels than shore-oblique wavefronts. The role of refraction phenomena driven by nearshore morphology is of great importance in this respect, so visual evidence of wave approach directions should be used where possible. In the present work, this parameter has been established considering the wave attack angle of the most important storm. The approaching angle was evaluated in a quantitative way following the intervals proposed by García-Mora et al. [82].

(D) Relative Sea Level trend: Despite the impact of relative sea-level trend, it is less important than other factors in determining cliff erosion susceptibility [84], although it must be considered when evaluating potential cliff erosion since it is one of the main effects of climate change. Considering the recent estimates about accelerating sea-level rise [85], it is clear that the importance of relative sea-level change in a given area will depend on the considered time-span. In this paper were obtained IPCC data from the SSP2-4.5 scenario presented by NASA [86], which predicted SLR is in line with the upper end of aggregate Nationally Determined Contribution emission levels by 2030. It deviates slightly from a no-additional-climate-policy reference scenario, resulting in a best-estimate warming of approximately 2.7 °C by the end of the 21st century relative to the years 1850–1900. It is important to emphasize that these databases provide data in absolute values that must be corrected, considering the continent uplift values and local/regional subsidence, i.e., in this case local/regional data [87,88]. Table 3 shows the classes and ranking criteria adopted for each variable of the forcing index.

**Table 3.** Coastal Forcing Index rating from 1 – minimum (green) to maximum (red) forcing values.

Parameter	RATING			Weight
	Low/Null (1)	Medium (2)	High (3)	
Significant wave height at a specific coastal sector (% of initial $H_s$ )	$H_s \leq 20\%$	$20\% < H_s \leq 60\%$	$60\% < H_s \leq 100\%$	1
Tidal range	Macrotidal ( $T_d \geq 4$ m)	Mesotidal ( $4 < T_d \leq 2$ m)	Microtidal ( $T_d < 2$ m)	0.5
Degree of littoral exposition to wave fronts	$45^\circ \leq \alpha < 10^\circ$ Oblique	$10^\circ \leq \alpha < 5^\circ$ Subparallel	$5^\circ \leq \alpha < 0^\circ$ Parallel	0.8
Relative Sea level trend <sup>1</sup>	Fall/Stable (Rising lower than the average value at regional scale <sup>2</sup> )	Rising (Rising equal to average local trend at regional scale)	Highly rising (Rising higher than the average local trend at the regional scale)	0.5

Notes: <sup>1</sup> Estimation expected by the end of the century (2100). <sup>2</sup> Regional values are from the IPCC SSP2-4.5 scenario and are corrected by taking local land movement data into account.

The scores of each variable have been summed in order to obtain an absolute value for the index by using Equation (2):

$$CFI_x = \sum_{i=1}^n \frac{C_i * W_{Fi}}{nCFI} \quad (2)$$

where  $C_i$  is the forcing value,  $W_{Fi}$  is the weight factor and  $nCFI$  is the number of variables considered in the index assessment. Table 4 shows the obtained five classes of forcing, ranging between 0 and 3.5.

**Table 4.** The obtained five Forcing Index classes indicating – from green to red – an increase of forcing agents impact.

Class	Value	
Null/Very low	$0 < CFI_x \leq 0.7$	
Low	$0.7 < CFI_x \leq 1.4$	
Medium	$1.4 < CFI_x \leq 2.1$	
High	$2.1 < CFI_x \leq 2.8$	
Very high	$2.8 < CFI_x \leq 3.5$	

### 3.3. Susceptibility Evaluation

Finally, a Susceptibility Index has been created representing the probability of occurrence of a potentially damaging phenomenon within a given area. In other words, this index shows the potential of the considered sector to experience significant damages associated with the effect of forcing agents. It is the result of the crossing of the Forcing and Physical Elements Indexes, as evidenced in Equation (3):

$$CSI_x = \frac{(PEI * nPEI) + (CFI * nCFI)}{(nPEI + nCFI)} \quad (3)$$

Table 5 shows the obtained five classes of Susceptibility ranging from 0 and 3.1.

**Table 5.** The obtained five Coastal Susceptibility Index classes indicating – from green to red- an increase of cliff susceptibility.

Class	Value	
Null/Very low	$0 < CSI_x \leq 0.62$	
Low	$0.62 < CSI_x \leq 1.24$	
Medium	$1.24 < CSI_x \leq 1.86$	
High	$1.86 < CSI_x \leq 2.48$	
Very high	$2.48 < CSI_x \leq 3.1$	

### 3.4. Index Validation

As suggested by Cooper & McLaughlin [10], new methodological approaches to susceptibility and hazard assessment should be tested and validated before being considered as appropriate for their purposes. For this reason, the validity of the susceptibility index proposed in this work was tested through real cliff erosion data recorded in the Cilento and Procida areas. These data consisted of cliff recession rates derived from a series of aerial orthophotographs at scales 1:10,000, dating from 1988/1989 and Google Earth images of the year 2021.

Firstly, the cliff top was digitized on the orthophotographs and the above-mentioned images, except on those cliffed sections characterized by densely vegetated edges where the cliff foot was considered [89,90]. The traced shorelines were then compared in an ArcGIS environment 10.4, being the use of GIS tools accepted as the most common way of deriving coastal risk or vulnerability indices [10,91]. Their use allow to accelerate the spatial analysis operations, interpolations, and the integration of data from different sources, facilitating the information update.

After the acquisition of the two coastlines, the cliff recession rates were calculated by using the area-based analysis (ABA) method [92–94] instead of the commonly used transect-from-baseline (TBA) method. In particular, the ABA method uses two separate coastlines to build a polygon topology that represents the total areal difference between the two coastlines. It computes the mean shoreline displacement for the identified coastal segment by dividing the cliff (or beach) area variation, i.e., the area between the two coastlines, by the segment length, i.e., the average length of the two used shorelines [93], providing the mean displacement for the considered study sector [94–96].

Normally, both ABA and TBA methods can be easily applied in the retreat rate evaluation, but ABA needs a coastline position acquired in continuity or with very close points, whereas TBA can be based on spaced transect data. Transects are taken as representative of a coastal sector, but their position does not necessarily fall in its most representative points (this is especially a problem in the presence of megacusps and/or human protection structures), while when using the area-based analysis, each infinitesimal coastal segment gives its contribution to the dry beach planform assessment, making this method more reliable. By using this approach, the entire surface between the two considered coastlines is quantified, and all portions of both coastlines are used in the area computation.

#### 4. Results and Discussion

The method proposed in this study was applied at 20 cliffed sectors located along the Mediterranean coast of the Cilento and Procida areas. The variables in Tables 2 and 3 were carefully evaluated for each sector by field surveys and the analysis of bibliographic data. Figure 3 shows all of the cliffed sectors analyzed in this study.

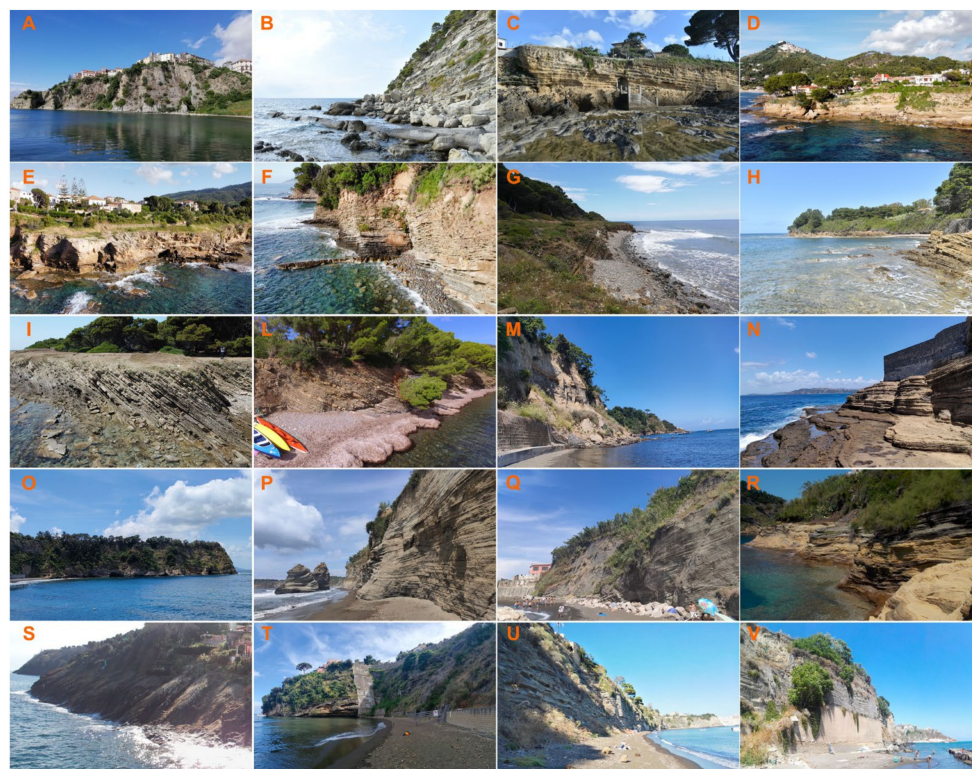


**Figure 3.** Studied cliffs along the Cilento area (A–L) and Procida Island (M–V).

##### 4.1. Physical Elements Index ( $PEI_x$ )

The Cilento area was mainly classified inside the “High” class of proneness, since 60% of the analyzed sectors show values ranging between 1.8 and 2.4. This is the case of the Pozzilli and San Marco di Castellabate sites (Figure 3C–E), a series of high cliffs characterized by slope values  $> 61^\circ$ , highly weathered rocks with an elevated percentage of discontinuities [23], and no protection structures at the cliff base. “Medium”  $PEI_x$  values were recorded in 30% of the cases, where investigated sectors show  $PEI_x$  values between 1.2 and 1.8, such as in the case of Torre di Mezzo and Punta Ogliastro (Figure 3H,I,L), where low coastal height (between 6 and 22 m), composed of stratified sandstones, are protected by a wide platform at the cliff base, a parameter that improves the score obtained within this index. Only 10% of the cases in Cilento show a “Low” value of susceptibility, with  $PEI_x$  values between 0.7 and 1.2. This is the case of Punta Licosa (Figure 3G), where low-height cliffs with a low slope are protected by a wide platform at the cliff base. All of the sectors analyzed along the Procida coastline register “High” values of proneness, with values ranging between 1.8 and 2.4, mainly due to the poor morphometrical and geomechanical features (i.e., height, slope, lithology, percentage of discontinuities and erosional features). An example of graphical representations of  $PEI_x$  collected data can be found in Figure A1 (Appendix A).

##### 4.2. Coastal Forcing Index ( $CFI_x$ )

In the Cilento area, the investigated cliffed sectors showed “High” to “Very high” values of  $CFI_x$ ; 50% of the analyzed areas showed “Very high” values of  $CFI_x$ , e.g., in the case of San Marco and Torre di Mezzo sites (Figure 3D,H), while the remaining 50% showed

“High” values of  $CFI_x$ , e.g., the case of the Agropoli and Punta Tresino sites (Figure 3A,B). The obtained data suggest that the prevalence of high coastal forcing is related to the conjunction of several factors determining the way in which wave energy is distributed along the coastline, such as the high wave height at the cliff foot, the exposition of the littoral to waves and the presence of a microtidal regime. In particular, cliff orientation determines the level of exposure to the waves’ fronts and, consequently, the arrival of very energetic waves. However, the very higher values of forcing obtained along Punta Licosa Promontory with respect to other parts of Cilento are linked to the greater exposition of this coast, as it is parallel to the incoming wave fronts mainly approaching from the WSW. Procida Island shows a “Medium” to “Very high” value of CFI, while medium values were observed in 10% of the cases, e.g., at the Ciracciello sector (Figure 3Q), where the significant wave height at the cliff base is lower than 20% of the initial  $H_s$ , mainly due to the presence of protection structures at the cliff foot. “High” values of  $CFI_x$  were observed in 60% of cases, mainly due to the significant wave height at the cliff foot which is comprised between 20 and 60%, and to the subparallel exposition to the waves’ fronts. “Very high” values of  $CFI_x$  were observed in the remaining 20%, i.e., at Ciraccio and Solchiaro (Figure 3P,S) mainly due to coastal orientation that is parallel to the main waves’ fronts. An example of graphical representations of  $CFI_x$  can be found in Figure A2 (Appendix B).

#### 4.3. Cliff Susceptibility Index ( $CSI_x$ )

In the Cilento area, “Medium” to “High” values of susceptibility were registered. High values are dominant, accounting for 60% of the analyzed area, especially in the northern part of the study area. “Medium Values” accounted for 40% of the coastline, occurring in the southern part of the study area. However, no low or null hazard values have been observed along the Cilento sector. Along the Procida coastal area, “High” and “Very high” values of susceptibility have been observed, mainly due to the poor geomechanical features of the material that constitutes the cliffs, as well as the high exposure to meteo-marine forcing. Specifically, “Very high” values of susceptibility (20%) were observed at the Ciraccio and Chiaia 2 sectors, while high values were observed in all of the remaining analyzed sectors. In the case of Procida, no “Low” or “Null”  $CSI_x$  values have been observed. The main characteristics and results of the susceptibility analysis in the two areas are presented in Table 6, and Figure 4 shows the susceptibility map of high coastal sectors along the Cilento and Procida areas.

**Table 6.** Main characteristics of the study sectors in the Cilento (C) and Procida (P) areas, classified by sites, municipality, Physical Elements Index ( $PEI_x$ ), Forcing Index ( $CFI_x$ ), Susceptibility Index ( $CSI_x$ ) and Susceptibility Class ( $CSI_x$  Class). Colors according to Table 5.

Area	Site	Municipality	$PEI_x$	$CFI_x$	$CSI_x$	$CSI$ Class
C	Agropoli	Agropoli	1.90	2.60	2.04	
C	Punta Tresino	Agropoli	2.00	2.70	2.14	
C	Pozzilli	Castellabate	2.10	2.70	2.22	
C	San Marco 1	Castellabate	2.10	3.10	2.22	
C	San Marco 2	Castellabate	2.10	3.10	2.22	
C	Acqua di Cesare	Castellabate	2.00	2.70	2.14	
C	Punta Licosa	Castellabate	1.20	3.50	1.74	
C	Torre di Mezzo	Castellabate	1.54	3.10	1.85	
C	Punta Ogliaastro 1	Castellabate	1.56	3.08	1.86	
C	Punta Ogliaastro 2	Castellabate	1.40	2.70	1.66	
P	Silurenza	Procida	2.10	2.70	2.22	
P	Punta Pioppeto	Procida	1.90	2.70	2.06	
P	Punta Serra	Procida	2.20	2.70	2.30	
P	Ciraccio	Procida	2.22	3.52	2.48	
P	Ciracciello	Procida	2.10	2.70	2.22	
P	Chiaiolella	Procida	2.00	2.20	2.04	
P	Solchiaro	Procida	2.08	3.00	2.26	
P	Chiaia 1	Procida	2.30	2.20	2.28	
P	Chiaia 2	Procida	2.44	2.70	2.49	
P	Chiaia 3	Procida	2.11	2.70	2.23	

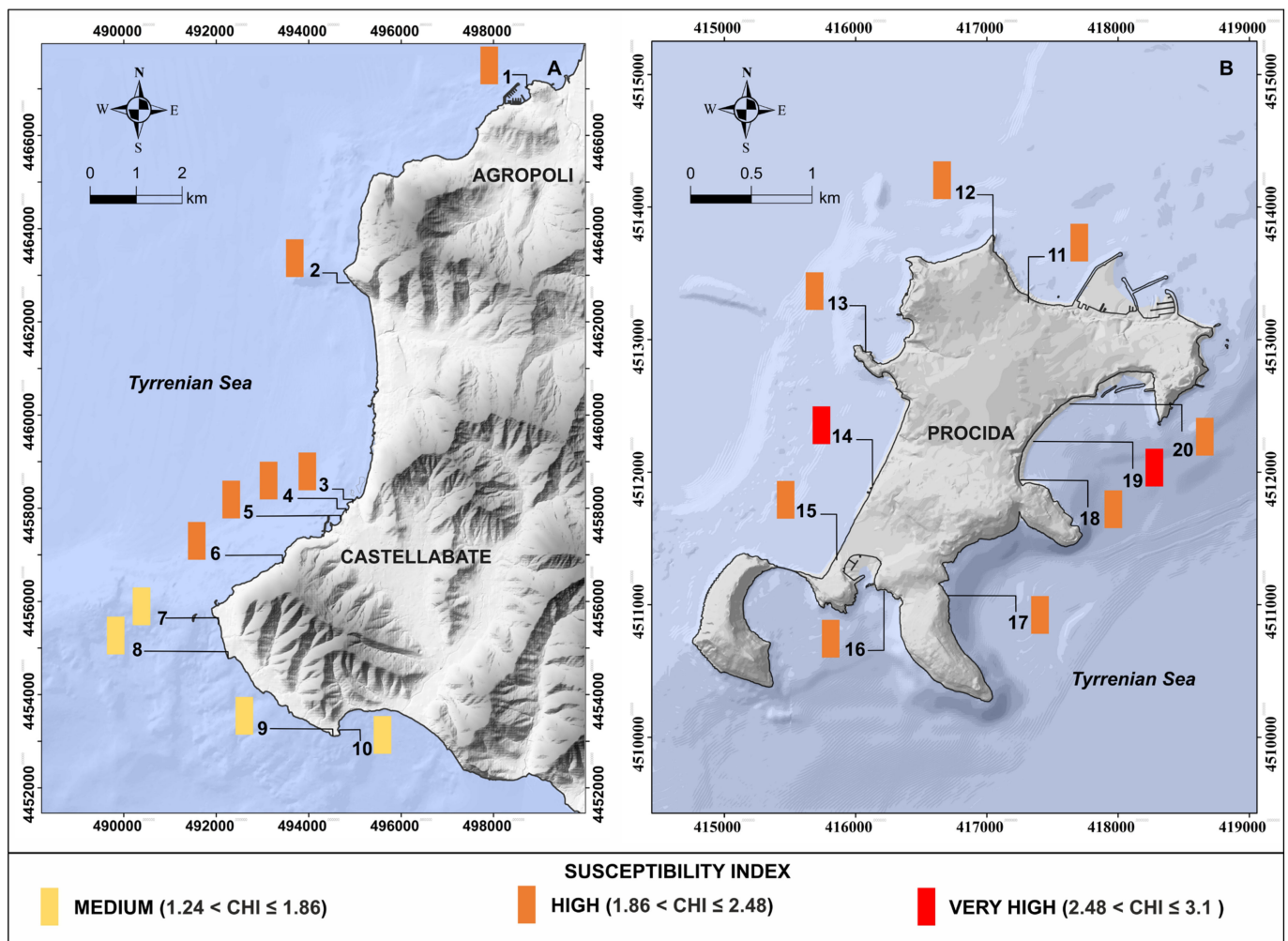


**Figure 4.** Susceptibility map of high coastal sectors along the Cilento area (A) and Procida area (B). Numbers indicate the study sites.

#### 4.4. Index Validation

As mentioned in Section 3.4, new approaches for susceptibility assessment should be validated and tested before being considered to be appropriate for their specific purposes [10]. After the calculation of the retreating rate, reported in Table A1 (Appendix C), through the ABA method, the linear multiple regression (LMR) was used for each analysed cliffed sector to evaluate the existing correlation between the calculated Cliff Susceptibility Index (CSI) and Cliff Retreat Rate (RR).

The LMR is a statistical technique that predicts the values assumed by a dependent variable from the knowledge of the values observed on several independent variables.

In this case, the relation was evaluated according to the following expression:

$$CSI = f(RR) \tag{4}$$

This model includes the output data, such as  $R^2$ , to provide information on the accuracy of the model's estimation of the dependent variable. Small differences between the expected and observed values indicate that the model fits the data well. On the contrary, significant differences between expected and observed values indicate that the model does not explain data variability well. Results of this validation are presented in Table 7, and show an acceptable correlation according to the  $R^2$  coefficient, with around 77% of the variation in the CSI being explained by the model.

**Table 7.** CSI: Cliff Susceptibility Index. Multiple R: Multiple correlation coefficient. Multiple R<sup>2</sup>: Coefficient of multiple determination. Adjusted R<sup>2</sup>: Coefficient of determination adjusted by the number of independent variables.

CSI = f(RR)	
Multiple R	0.87
Multiple R <sup>2</sup>	0.77
Adjusted R <sup>2</sup>	0.75

According to Del Río & Gracia [1], if the value of the Cliff Susceptibility Index is not in accordance with coastal evolution data, it is possible that other relevant factors not considered in the index are influencing coastline erosion. As this was not the case, it is possible to state that the proposed Susceptibility Index represents a valid approach to the estimation of cliff erosion susceptibility.

## 5. Methodological Considerations and Concluding Remarks

Cliff erosion processes, which represent the main hazard in rocky environments, have been evaluated in this paper through an index-based method, developed to be a scientific planning tool that takes into account a higher number of factors involved in the determination of hazards related to erosion.

This aims to be an easy-to-use, general and non-site-specific tool, consisting of a simple set of indices applicable to different high coastal areas. Special attention in this kind of assessment has to be devoted to the scale of work due to the spatial resolution of the zoning used.

Given that susceptibility evaluations have to be assessed for coastal management purposes, spatial resolution of the segmentation must be in accordance with the level at which it is planned in order to support stakeholders and management decision-making at local, regional or national scales. The method does not introduce a score based on the magnitude and frequency of specific events, but it provides a grade of proneness, with classes ranging from 1 to 5, where 1 indicates low susceptibility and 5 very high susceptibility.

The Susceptibility Index was validated by using real cliff erosion data from the Cilento and Procida coast in southern Italy. The Cilento high coast has 40% of its length within the “Medium” susceptibility class (Class 3) and 60% in the “High” susceptibility class (Class 4). Concerning Procida Island, 80% of cliffs fall into the “High” susceptibility class (Class 4), and 20% in the “Very high” susceptibility class (Class 5). These results suggest that the greater parts of the studied cliff, especially those in Class 5, require special attention and local management protection strategies in order to decrease their susceptibility and their exposure to forcing agents.

Finally, the proposed Susceptibility Index should be tested versus cliff recession data in other locations in order to validate it in diverse coastal settings, e.g., cliffs composed of metamorphic rocks or in meso- and macro-tidal environments.

**Author Contributions:** M.F.T. and G.A. designed the study and participated in all phases. G.M., F.M. and P.P.C.A. provided a global structural discussion and participated in the development of the methodological approach. M.F.T., G.A. and F.M. carried out the fieldwork observations and analysed the results. G.M. and P.P.C.A. made contributions regarding the conceptual approach. All authors have read and agreed to the published version of the manuscript.

**Funding:** This research received no external funding.

**Institutional Review Board Statement:** Not applicable.

**Informed Consent Statement:** Not applicable.

**Data Availability Statement:** Not applicable.

**Conflicts of Interest:** The authors declare that they have no conflicts of interest.

### Appendix A

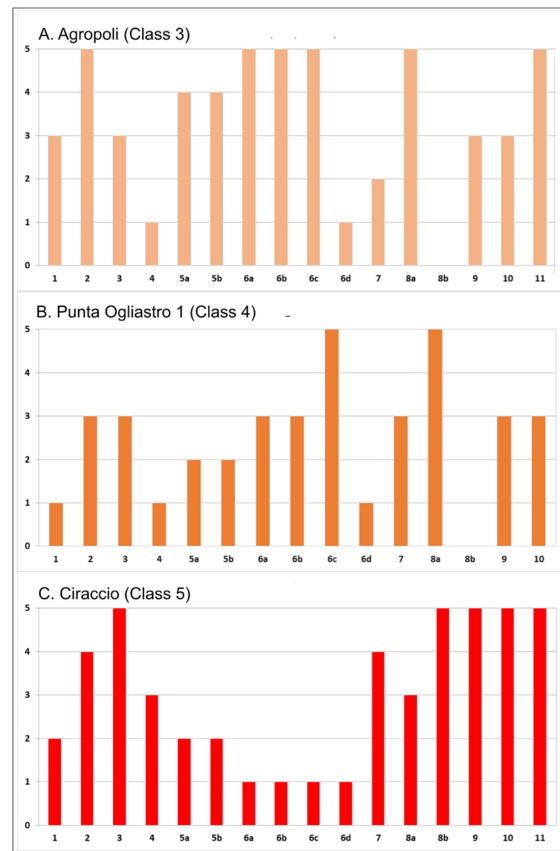


**Figure A1.** Graphical representations of the PELx collected data. (A) Agropoli (Class 3); (B) Punta Ogliastro 1 (Class 4); (C) Ciraccio (Class 5).

### Appendix B

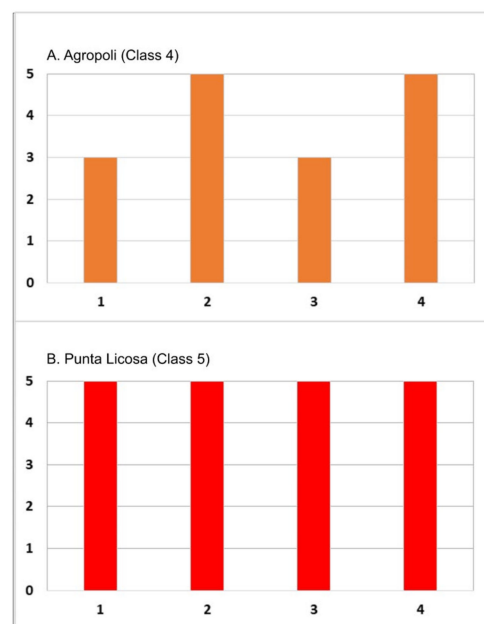


**Figure A2.** Graphical representations of the CFI collected data. (A) Agropoli (Class 4); (B) Punta Licosa (Class 5).

## Appendix C

**Table A1.** Values of the Cliff Retreat Rate (RR) from 1989 to 2021 of analyzed high coastal sectors.

Site	Retreat Rate (RR)
Agropoli	3.3 m
Punta Tresino	3.5 m
Pozzilli	3.7 m
San Marco 1	4.1 m
San Marco 2	5.1 m
Acqua di Cesare	4.6 m
Punta Licosa	2.3 m
Torre di Mezzo	2.2 m
Punta Ogliastro 1	3.1 m
Punta Ogliastro 2	2.9 m
Silurenza	6.0 m
Punta Pioppeto	Not evaluable
Punta Serra	4.9 m
Ciraccio	6.7 m
Ciracciello	7.1 m
Chiaiolella	1.8 m
Solchiaro	3.0 m
Chiaia 1	Not evaluable
Chiaia 2	6.5 m
Chiaia 3	4.8 m

## References

- Del Río, L.; Gracia, F.J. Erosion Risk Assessment of Active Coastal Cliffs in Temperate Environments. *Geomorphology* **2009**, *112*, 82–95. [[CrossRef](#)]
- Emery, K.O.; Kuhn, G.G. Sea Cliffs: Their Processes, Profiles, and Classification. *Geol. Soc. Am. Bull.* **1982**, *93*, 644–654. [[CrossRef](#)]
- Trenhaile, A.S. *The Geomorphology of Rock Coasts*; Oxford University Press: Oxford, UK, 1987.
- Doody, P.; Office for Official Publications of the European Communities (Eds.) *Living with Coastal Erosion in Europe: Sediment and Space for Sustainability*; Publications Office of the European Communities: Luxembourg, 2004; ISBN 978-92-894-7496-2.
- Trenhaile, A.S. Chapter 2 Climate Change and Its Impact on Rock Coasts. *Memoirs* **2014**, *40*, 7–17. [[CrossRef](#)]
- Hampton, M.A.; Griggs, G.B.; Edil, T.B.; Guy, D.E.; Kelley, J.T.; Komar, P.D.; Mickelson, D.M.; Shipman, H.M. Processes That Govern the Formation and Evolution of Coastal Cliffs. *US Geol. Surv. Prof. Pap.* **2004**, *1693*, 7–38.
- Teixeira, S.B. Slope Mass Movements on Rocky Sea-Cliffs: A Power-Law Distributed Natural Hazard on the Barlavento Coast, Algarve, Portugal. *Continent. Shelf Res.* **2006**, *26*, 1077–1091. [[CrossRef](#)]
- Trenhaile, A.S. Rock Coasts, with Particular Emphasis on Shore Platforms. *Geomorphology* **2002**, *48*, 7–22. [[CrossRef](#)]
- Naylor, L.A.; Stephenson, W.J.; Trenhaile, A.S. Rock Coast Geomorphology: Recent Advances and Future Research Directions. *Geomorphology* **2010**, *114*, 3–11. [[CrossRef](#)]
- Cooper, J.A.G.; McLaughlin, S. Contemporary Multidisciplinary Approaches to Coastal Classification and Environmental Risk Analysis. *J. Coast. Res.* **1998**, *14*, 512–524.
- Williams, A.T.; Alveirinho-Dias, J.; Novo, F.G.; Garcia-Mora, M.R.; Curr, R.; Pereira, A. Integrated Coastal Dune Management: Checklists. *Continent. Shelf Res.* **2001**, *21*, 1937–1960. [[CrossRef](#)]
- Pappone, G.; Aucelli, P.P.C.; Aberico, I.; Amato, V.; Antonioli, F.; Cesarano, M.; Di Paola, G.; Pelosi, N. Relative Sea-Level Rise and Marine Erosion and Inundation in the Sele River Coastal Plain (Southern Italy): Scenarios for the next Century. *Rend. Lincei* **2012**, *23*, 121–129. [[CrossRef](#)]
- Aucelli, P.P.C.; Di Paola, G.; Incontri, P.; Rizzo, A.; Vilardo, G.; Benassai, G.; Buonocore, B.; Pappone, G. Coastal Inundation Risk Assessment Due to Subsidence and Sea Level Rise in a Mediterranean Alluvial Plain (Volturno Coastal Plain–Southern Italy). *Estuar. Coast. l Shelf Sci.* **2017**, *198*, 597–609. [[CrossRef](#)]
- Rizzo, A.; Aucelli, P.P.C.; Gracia, F.J.; Anfuso, G. A Novelty Coastal Susceptibility Assessment Method: Application to Valdela-grana Area (SW Spain). *J. Coast. Conserv.* **2018**, *22*, 973–987. [[CrossRef](#)]
- Mattei, G.; Rizzo, A.; Anfuso, G.; Aucelli, P.P.C.; Gracia, F.J. A Tool for Evaluating the Archaeological Heritage Vulnerability to Coastal Processes: The Case Study of Naples Gulf (Southern Italy). *Ocean Coast. Manag.* **2019**, *179*, 104876. [[CrossRef](#)]
- Crowell, M.; Honeycutt, M.; Hatheway, D. Coastal Erosion Hazards Study: Phase One Mapping. *J. Coast. Res.* **1999**, *28*, 10–20.
- Anfuso, G.; Martínez Del Pozo, J.Á. Assessment of Coastal Vulnerability through the Use of GIS Tools in South Sicily (Italy). *Environ. Manag.* **2009**, *43*, 533–545. [[CrossRef](#)] [[PubMed](#)]

18. Mclaughlin, S.; Cooper, J.A.G. A Multi-Scale Coastal Vulnerability Index: A Tool for Coastal Managers? *Environ. Hazards* **2010**, *9*, 233–248. [[CrossRef](#)]
19. Rangel-Buitrago, N.; Anfuso, G. *Risk Assessment of Storms in Coastal Zones: Case Studies from Cartagena (Colombia) and Cadiz (Spain)*; Springer: Cham, Switzerland, 2015. [[CrossRef](#)]
20. Richmond, B.M.; Fletcher III, C.H.; Grossman, E.E.; Gibbs, A.E. Islands at Risk: Coastal Hazard Assessment and Mapping in the Hawaiian Islands. *Environ. Geosci.* **2001**, *8*, 21–37. [[CrossRef](#)]
21. De Pippo, T.; Donadio, C.; Pennetta, M.; Petrosino, C.; Terlizzi, F.; Valente, A. Coastal Hazard Assessment and Mapping in Northern Campania, Italy. *Geomorphology* **2008**, *97*, 451–466. [[CrossRef](#)]
22. Anfuso, G.; Postacchini, M.; Di Luccio, D.; Benassai, G. Coastal Sensitivity/Vulnerability Characterization and Adaptation Strategies: A Review. *J. Mar. Sci. Eng.* **2021**, *9*, 72. [[CrossRef](#)]
23. Budetta, P.; Santo, A.; Vivenzio, F. Landslide Hazard Mapping along the Coastline of the Cilento Region (Italy) by Means of a GIS-Based Parameter Rating Approach. *Geomorphology* **2008**, *94*, 340–352. [[CrossRef](#)]
24. Matano, F.; Iuliano, S.; Somma, R.; Marino, E.; del Vecchio, U.; Esposito, G.; Molisso, F.; Scepi, G.; Grimaldi, G.M.; Pignalosa, A. Geostructure of Coroglio Tuff Cliff, Naples (Italy) Derived from Terrestrial Laser Scanner Data. *J. Maps* **2016**, *12*, 407–421. [[CrossRef](#)]
25. Caputo, T.; Marino, E.; Matano, F.; Somma, R.; Troise, C.; De Natale, G. Terrestrial Laser Scanning (TLS) Data for the Analysis of Coastal Tuff Cliff Retreat: Application to Coroglio Cliff, Naples, Italy. *Ann. Geophys.* **2018**, *61*, SE110. [[CrossRef](#)]
26. Esposito, G.; Salvini, R.; Matano, F.; Sacchi, M.; Troise, C. Evaluation of Geomorphic Changes and Retreat Rates of a Coastal Pyroclastic Cliff in the Campi Flegrei Volcanic District, Southern Italy. *J. Coast. Conserv.* **2018**, *22*, 957–972. [[CrossRef](#)]
27. Esposito, G.; Matano, F.; Sacchi, M.; Salvini, R. Mechanisms and Frequency-Size Statistics of Failures Characterizing a Coastal Cliff Partially Protected from the Wave Erosive Action. *Rend. Lincei. Sci. Fis. Nat.* **2020**, *31*, 337–351. [[CrossRef](#)]
28. Esposito, G.; Salvini, R.; Matano, F.; Sacchi, M.; Danzi, M.; Somma, R.; Troise, C. Multitemporal Monitoring of a Coastal Landslide through SfM-derived Point Cloud Comparison. *Photogramm. Rec.* **2017**, *32*, 459–479. [[CrossRef](#)]
29. De Vita, P.; Cevasco, A.; Cavallo, C. Detailed Rock Failure Susceptibility Mapping in Steep Rocky Coasts by Means of Non-Contact Geostructural Surveys: The Case Study of the Tigullio Gulf (Eastern Liguria, Northern Italy). *Nat. Hazards Earth Syst. Sci.* **2012**, *12*, 867–880. [[CrossRef](#)]
30. Di Luccio, D.; Aucelli, P.P.C.; Di Paola, G.; Pennetta, M.; Berti, M.; Budillon, G.; Florio, A.; Benassai, G. An Integrated Approach for Coastal Cliff Susceptibility: The Case Study of Procida Island (Southern Italy). *Sci. Total Environ.* **2023**, *855*, 158759. [[CrossRef](#)]
31. Lucchetti, A.; Brandolini, P.; Faccini, F.; Firpo, M. Proposta di valutazione della stabilità delle coste rocciose (SCMR—Sea Cliff Mass Rating): Il caso studio delle falesie tra Genova e Camogli (Liguria orientale). *Stud. Cost.* **2014**, *22*, 137–149.
32. Romana, M. New Adjustment Ratings for Application of Bieniawski Classification to Slopes. In Proceedings of the International Symposium on Role of Rock Mechanics, Zacatecas, Mexico, 1985; pp. 49–53.
33. Furlani, S.; Devoto, S.; Biolchi, S.; Cucchi, F. Factors Triggering Sea Cliff Instability Along the Slovenian Coasts. *J. Coast. Res.* **2011**, *61*, 387–393. [[CrossRef](#)]
34. Anfuso, G.; Gracia, F.J.; Battocletti, G. Determination of Cluffed Coastline Sensitivity and Associated Risk for Human Structures: A Methodological Approach. *J. Coast. Res.* **2013**, *29*, 1292. [[CrossRef](#)]
35. Bieniawski, Z.T. *Engineering Rock Mass Classifications: A Complete Manual for Engineers and Geologists in Mining, Civil, and Petroleum Engineering*; John Wiley & Sons: Hoboken, NJ, USA, 1989.
36. Marques, F.M.S.F.; Matildes, R.; Redweik, P. Sea Cliff Instability Susceptibility at Regional Scale: A Statistically Based Assessment in the Southern Algarve, Portugal. *Nat. Hazards Earth Syst. Sci.* **2013**, *13*, 3185–3203. [[CrossRef](#)]
37. Nunes, M.; Ferreira, Ó.; Schaefer, M.; Clifton, J.; Baily, B.; Moura, D.; Loureiro, C. Hazard Assessment in Rock Cliffs at Central Algarve (Portugal): A Tool for Coastal Management. *Ocean Coast. Manag.* **2009**, *52*, 506–515. [[CrossRef](#)]
38. Santangelo, N.; Amato, V.; Ascione, A.; Russo Ermolli, E.; Valente, E. Geotourism as a Tool for Learning: A Geoitinerary in the Cilento, Vallo Di Diano and Alburni Geopark (Southern Italy). *Resources* **2020**, *9*, 67. [[CrossRef](#)]
39. Guida, D.; Valente, A. Terrestrial and Marine Landforms along the Cilento Coastland (Southern Italy): A Framework for Landslide Hazard Assessment and Environmental Conservation. *Water* **2019**, *11*, 2618. [[CrossRef](#)]
40. Martelli, L.; Nardi, G.; Cammarosano, A.; Cavuoto, G.; Aiello, G.; D’Argenio, B.; Marsella, E. *Note Illustrative della Carta Geologica d’Italia (Scala 1: 50.000), Foglio 502 “Agropoli”*; Servizio Geologico d’Italia ISPRA: Rome, Italy, 2016; pp. 1–110.
41. Bonardi, G.; d’Argenio, B.; Perrone, V. Carta Geologica Dell’Appennino Meridionale Alla Scala 1: 250.000. *Mem. Della Soc. Geol. Ital.* **1988**, *41*.
42. Russo, M.; Zuppetta, A.; Guida, A. Alcune Precisazioni Stratigrafiche Sul Flysch Del Cilento (Appennino Meridionale). *Boll. Soc. Geol. Ital.* **1995**, *114*, 353–359.
43. Cammarosano, A.; Cavuoto, G.; Danna, M.; De Capoa, P.; De Rienzo, F.; Di Staso, A.; Giardino, S.; Martelli, L.; Nardi, G.; Sgrosso, A. Nuovi Dati e Nuove Interpretazioni Sui Flysch Terrigeni Del Cilento (Appennino Meridionale, Italia). *Boll. Soc. Geol. Ita.* **2004**, *119*, 395–405.
44. D’Argenio, B.; Aiello, G.; De Alteriis, G.; Milia, A.; Sacchi, M.; Tonielli, R.; Budillon, F.; Chiocci, F.L.; Conforti, A.; De Lauro, M. Digital Elevation Model of the Naples Bay and Adjacent Areas, Eastern Tyrrhenian Sea. In *Mapping Geology in Italy*; Pasquarè, G., Venturi, C., Gropelli, G., Eds.; APAT: Rome, Italy, 2004; Volume 3, pp. 21–28.

45. Ascione, A.; Aucelli, P.P.; Cinque, A.; Di Paola, G.; Mattei, G.; Ruello, M.; Russo Ermolli, E.; Santangelo, N.; Valente, E. Geomorphology of Naples and the Campi Flegrei: Human and Natural Landscapes in a Restless Land. *J. Maps* **2021**, *17*, 18–28. [[CrossRef](#)]
46. Putignano, M.L.; Schiattarella, M. Geomorfologia Strutturale e Domini Di Frattura Dei Fondali Marini Pericostieri Dell’Isola Di Procida (Campi Flegrei Insulari, Italia Meridionale). *Alp. Mediterr. Quat.* **2010**, *23*, 229–242.
47. Putignano, M.L.; Orrù, P.E.; Schiattarella, M. Holocene Coastline Evolution of Procida Island, Bay of Naples, Italy. *Quat. Int.* **2014**, *332*, 115–125. [[CrossRef](#)]
48. Aucelli, P.P.; Mattei, G.; Caporizzo, C.; Di Luccio, D.; Tursi, M.F.; Pappone, G. Coastal vs Volcanic Processes: Procida Island as a Case of Complex Morpho-Evolutive Response. *Mar. Geol.* **2022**, *448*, 106814. [[CrossRef](#)]
49. Sunamura, T. *Geomorphology of Rocky Coasts*; Wiley: Hoboken, NJ, USA, 1992.
50. Benumof, B.T.; Storlazzi, C.D.; Seymour, R.J.; Griggs, G.B. The Relationship between Incident Wave Energy and Seacliff Erosion Rates: San Diego County, California. *J. Coast. Res.* **2000**, *16*, 1162–1178.
51. Di Paola, G.D.; Iglesias, J.; Rodríguez, G.; Benassai, G.; Aucelli, P.; Pappone, G. Estimating Coastal Vulnerability in a Meso-Tidal Beach by Means of Quantitative and Semi-Quantitative Methodologies. *J. Coast. Res.* **2011**, *61*, 303–308. [[CrossRef](#)]
52. Maio, C.V.; Gontz, A.M.; Tenenbaum, D.E.; Berkland, E.P. Coastal Hazard Vulnerability Assessment of Sensitive Historical Sites on Rainsford Island, Boston Harbor, Massachusetts. *J. Coast. Res.* **2012**, *28*, 20–33. [[CrossRef](#)]
53. Villa, F.; McLeod, H. Environmental Vulnerability Indicators for Environmental Planning and Decision-Making: Guidelines and Applications. *Environ. Manag.* **2002**, *29*, 335–348. [[CrossRef](#)]
54. Gornitz, V.M.; Daniels, R.C.; White, T.W.; Birdwell, K.R. The Development of a Coastal Risk Assessment Database: Vulnerability to Sea-Level Rise in the US Southeast. *J. Coast. Res.* **1994**, *12*, 327–338.
55. Rygel, L.; O’Sullivan, D.; Yarnal, B. A Method for Constructing a Social Vulnerability Index: An Application to Hurricane Storm Surges in a Developed Country. *Mitig. Adaptat. Strateg. Glob. Change* **2006**, *11*, 741–764. [[CrossRef](#)]
56. Gerivani, H.; Stephenson, W.; Afarin, M. Sea Cliff Instability Hazard Assessment for Coastal Management in Chabahar, Iran. *J. Coast Conserv.* **2020**, *24*, 5. [[CrossRef](#)]
57. Montoya-Montes, I.; Rodríguez-Santalla, I.; Sánchez-García, M.J.; Alcántara-Carrió, J.; Martín-Velázquez, S.; Gómez-Ortiz, D.; Martín-Crespo, T. Mapping of Landslide Susceptibility of Coastal Cliffs: The Mont-Roig Del Camp Case Study. *Geol. Acta* **2012**, *10*, 439–455.
58. Bush, D.M.; Neal, W.J.; Young, R.S.; Pilkey, O.H. Utilization of Geoinicators for Rapid Assessment of Coastal-Hazard Risk and Mitigation. *Ocean Coast. Manag.* **1999**, *42*, 647–670. [[CrossRef](#)]
59. Hoek, E.; Marinos, P.; Benissi, M. Applicability of the Geological Strength Index (GSI) Classification for Very Weak and Sheared Rock Masses. The Case of the Athens Schist Formation. *Bull. Eng. Geol. Environ.* **1998**, *57*, 151–160. [[CrossRef](#)]
60. Tsuguo, S. Processes of Sea Cliff and Platform Erosion. In *CRC Handbook of Coastal Processes and Erosion*; CRC Press: Boca Raton, USA, 2018; pp. 233–266.
61. Benumof, B.T.; Griggs, G.B. The Dependence of Seacliff Erosion Rates on Cliff Material Properties and Physical Processes: San Diego County, California. *Shore Beach* **1999**, *67*, 29–41.
62. Terzaghi, K. Stability of Steep Slopes on Hard Unweathered Rock. *Géotechnique* **1962**, *12*, 251–270. [[CrossRef](#)]
63. Trenhaile, A.S. The Width of Shore Platforms in Britain, Canada, and Japan. *J. Coast. Res.* **1998**, *15*, 355–364.
64. Trenhaile, A.S. Predicting the Response of Hard and Soft Rock Coasts to Changes in Sea Level and Wave Height. *Clim. Change* **2011**, *109*, 599–615. [[CrossRef](#)]
65. Coelho, C.; Granjo, M.-J.; Segurado-Silva, C. Map of Coastal Zone Vulnerabilities to Wave Actions Application to Aveiro District (Portugal). In *Integrated Coastal Zone Management*; Moksness, E., Dahl, E., Stttrup, J., Eds.; Wiley-Blackwell: Oxford, UK, 2009; pp. 318–330.
66. Mooser, A.; Anfuso, G.; Williams, A.T.; Molina, R.; Aucelli, P.P.C. An Innovative Approach to Determine Coastal Scenic Beauty and Sensitivity in a Scenario of Increasing Human Pressure and Natural Impacts Due to Climate Change. *Water* **2020**, *13*, 49. [[CrossRef](#)]
67. Short, A.D. *Handbook of Beach and Shoreface Morphodynamics*; John Wiley and Sons: Hoboken, NJ, USA, 1999.
68. Castedo, R.; Paredes, C.; de la Vega-Panizo, R.; Santos, A.P. The Modelling of Coastal Cliffs and Future Trends. In *Hydro-Geomorphology—Models and Trends*; Shukla, D.P., Ed.; InTech: London, UK, 2017.
69. Collins, B.D.; Sitar, N. Processes of Coastal Bluff Erosion in Weakly Lithified Sands, Pacifica, California, USA. *Geomorphology* **2008**, *97*, 483–501. [[CrossRef](#)]
70. Quinn, J.D.; Rosser, N.J.; Murphy, W.; Lawrence, J.A. Identifying the Behavioural Characteristics of Clay Cliffs Using Intensive Monitoring and Geotechnical Numerical Modelling. *Geomorphology* **2010**, *120*, 107–122. [[CrossRef](#)]
71. Aybulatov, N.A.; Artyukhin, Y.V. *Geo-Ecology of the World Ocean’s Shelf and Coasts*; Hydrometeo Publishing: Saint Petersburg, Russia, 1993.
72. Ergin, A.; Karaesmen, E.; Micallef, A.; Williams, A.T. A New Methodology for Evaluating Coastal Scenery: Fuzzy Logic Systems. *Area* **2004**, *36*, 367–386. [[CrossRef](#)]
73. Hartmann, D. Drowning and Beach-Safety Management (BSM) along the Mediterranean Beaches of Israel—A Long-Term Perspective. *J. Coast. Res.* **2006**, *22*, 1505–1514. [[CrossRef](#)]

74. Lee, E.M.; Hall, J.W.; Meadowcroft, I.C. Coastal Cliff Recession: The Use of Probabilistic Prediction Methods. *Geomorphology* **2001**, *40*, 253–269. [[CrossRef](#)]
75. Brown, S.; Barton, M.E.; Nicholls, R.J. The Effect of Coastal Defences on Cliff Top Retreat along the Holderness Coastline. *Proc. Yorks. Geol. Soc.* **2012**, *59*, 1–13. [[CrossRef](#)]
76. Gornitz, V.M.; Beaty, T.W.; Daniels, R.C. *A Coastal Hazards Data Base for The US West Coast*; Environmental Sciences Division Publication No. 4590; National Technical Information Service: Oak Ridge, TN, USA, 1997.
77. Mediterranean Sea Waves Forecasting System (Med-Waves). Available online: [https://resources.marine.copernicus.eu/productdetail/MEDSEA\\_MULTIYEAR\\_WAV\\_006\\_012/](https://resources.marine.copernicus.eu/productdetail/MEDSEA_MULTIYEAR_WAV_006_012/) (accessed on 15 September 2022).
78. European Centre for Medium-Range Weather Forecasts (ECMWF). Available online: <https://www.ecmwf.int/> (accessed on 10 November 2022).
79. Almeida, L.P.; Ferreira, Ó.; Vousedoukas, M.I.; Dodet, G. Historical Variation and Trends in Storminess along the Portuguese South Coast. *Nat. Haz. Earth System Sci.* **2011**, *11*, 2407–2417. [[CrossRef](#)]
80. Rangel-Buitrago, N.; Anfuso, G. Winter Wave Climate, Storms and Regional Cycles: The SW Spanish Atlantic Coast. *Int. J. Climatol.* **2013**, *33*, 2142–2156. [[CrossRef](#)]
81. Gornitz, V. Global Coastal Hazards from Future Sea Level Rise. *Palaeogeogr. Palaeoclimatol. Palaeoecol.* **1991**, *89*, 379–398. [[CrossRef](#)]
82. García-Mora, M.R.; Gallego-Fernández, J.B.; Williams, A.T.; García-Novo, F. A coastal dune vulnerability classification. *A case study of the SW Iberian Peninsula. J. Coast. Res.* **2001**, *17*, 802–811.
83. Komar, P. *Beach Processes and Sedimentation*; Prentice Hall: Upper Saddle River, NJ, USA, 1998.
84. Lee, E.M. Coastal Cliff Behaviour: Observations on the Relationship between Beach Levels and Recession Rates. *Geomorphology* **2008**, *101*, 558–571. [[CrossRef](#)]
85. Shukla, P.; Skea, J.; Slade, R.; Al Khourdajie, A.; van Diemen, R.; McCollum, D.; Pathak, M.; Some, S.; Vyas, P.; Fradera, R.; et al. (Eds.) *IPCC, 2022: Climate Change 2022: Mitigation of Climate Change. Contribution of Working Group III to the Sixth Assessment Report of the Intergovernmental Panel on Climate Change*; Cambridge University Press: Cambridge, UK; New York, NY, USA, 2022. [[CrossRef](#)]
86. NASA, Sea Level Projections tool. Available online: <https://sealevel.nasa.gov/ipcc-ar6-sea-level-projection-tool> (accessed on 13 July 2022).
87. Vilardo, G.; Ventura, G.; Terranova, C.; Matano, F.; Nardò, S. Ground Deformation Due to Tectonic, Hydrothermal, Gravity, Hydrogeological, and Anthropogenic Processes in the Campania Region (Southern Italy) from Permanent Scatterers Synthetic Aperture Radar Interferometry. *Remote Sens. Environ.* **2009**, *113*, 197–212. [[CrossRef](#)]
88. Matano, F. Analysis and Classification of Natural and Human-Induced Ground Deformations at Regional Scale (Campania, Italy) Detected by Satellite Synthetic-Aperture Radar Interferometry Archive Datasets. *Remote Sens. Environ.* **2019**, *11*, 2822. [[CrossRef](#)]
89. Moore, L.J.; Griggs, G.B. Long-Term Cliff Retreat and Erosion Hotspots along the Central Shores of the Monterey Bay National Marine Sanctuary. *Mar. Geol.* **2002**, *181*, 265–283. [[CrossRef](#)]
90. Pierre, G. Processes and Rate of Retreat of the Clay and Sandstone Sea Cliffs of the Northern Boulonnais (France). *Geomorphology* **2006**, *73*, 64–77. [[CrossRef](#)]
91. Garcia, G.M.; Pollard, J.; Rodriguez, R.D. Origins, Management, and Measurement of Stress on the Coast of Southern Spain. *Coast. Manage.* **2000**, *28*, 215–234. [[CrossRef](#)]
92. Smith, M.J.; Cromley, R.G. Measuring Historical Coastal Change Using GIS and the Change Polygon Approach: Measuring Historical Coastal Change. *Trans. GIS* **2012**, *16*, 3–15. [[CrossRef](#)]
93. Albuquerque, M.; Espinoza, J.; Teixeira, P.; de Oliveira, A.; Corrêa, I.; Calliari, L. Erosion or Coastal Variability: An Evaluation of the DSAS and the Change Polygon Methods for the Determination of Erosive Processes on Sandy Beaches. *J. Coast. Res.* **2013**, *165*, 1710–1714. [[CrossRef](#)]
94. Anfuso, G.; Bowman, D.; Danese, C.; Pranzini, E. Transect Based Analysis versus Area Based Analysis to Quantify Shoreline Displacement: Spatial Resolution Issues. *Environ. Monit. Assess.* **2016**, *188*, 568. [[CrossRef](#)]
95. Rogers, S.S.; Sandweiss, D.H.; Maasch, K.A.; Belknap, D.F.; Agouris, P. Coastal Change and Beach Ridges along the Northwest Coast of Peru: Image and GIS Analysis of the Chira, Piura, and Colan Beach-Ridge Plains. *J. Coast. Res.* **2004**, *20*, 1102–1125. [[CrossRef](#)]
96. Aminti, P.; Cammelli, C.; Cappietti, L.; Jackson, N.L.; Nordstrom, K.F.; Pranzini, E. Evaluation of Beach Response to Submerged Groin Construction at Marina Di Ronchi, Italy, Using Field Data and a Numerical Simulation Model. *J. Coast. Res.* **2004**, *33*, 99–120.

**Disclaimer/Publisher’s Note:** The statements, opinions and data contained in all publications are solely those of the individual author(s) and contributor(s) and not of MDPI and/or the editor(s). MDPI and/or the editor(s) disclaim responsibility for any injury to people or property resulting from any ideas, methods, instructions or products referred to in the content.